DEPARTMENT OF THE INTERIOR
UNITED STATES GEOLOGICAL SURVEY

MISCELLANEOUS FIELD STUDIES
MAP MF 1176-G
PAMPHLET

AEROMAGNETIC SURVEY AND INTERPRETATION OF THE SURVEY PASS QUADRANGLE, ALASKA

INTRODUCTION

This map was prepared as part of a multidisciplinary study of the geology and mineral resources of the Survey Pass quadrangle done under the auspices of the Alaska Mineral Resources Assessment Program (AMRAP). It is part of a folio of maps labeled MF-1176 A-I. Sheet 1 of the map is the aeromagnetic map. Sheet 2 is the "Magnetic Lineament and Anomaly Trend Map" by Steve W. Hackett of the Alaska Division of Geological and Geophysical Surveys (ADGGS). It bears its own descriptive text. Sheet 3 is the "Aeromagnetic-Interpretation Map" by John W. Cady of the U.S. Geological Survey and Steve W. Hackett of the ADGGS.

AEROMAGNETIC DATA

A 1:250,000-scale total-intensity aeromagnetic map was compiled from aeromagnetic surveys flown and compiled in 1974, 1975, and 1978 by Airborne Geophysics and GeoMetrics under contract to the Alaska Department of Natural Resources. Maps made from these surveys were published by the Alaska Division of Geological and Geophysical Surveys (ADGGS) in 1976 and 1979 at a scale of 1:63,000.

The aeromagnetic data were continuously recorded about 300 m above ground level along north-south flight lines spaced 1.2 km apart. Flight-line navigation and position were controlled by preliminary 1:63,360-scale topographic mapping and may contain some errors that affect the position of aeromagnetic anomalies. Radar altimetry data were continuously recorded for each flight path, but they were not used in the reduction of the aeromagnetic data. A regional trend based upon the 1965 International Geomagnetic Reference Field (IGRF), updated to 1975, was removed from the data that were taken in 1974 west of long 153°20'. A regional trend based upon the 1975 IGRF, updated to 1978, was removed from the data that were taken in 1978 east of long 153°20'. The magnetic data were processed and contoured on 1:63,360-scale maps and subsequently compiled (Hackett, 1977, revised 1980) to form the 1:250,000-scale aeromagnetic map. Contour intervals are at 10 and 100 gammas.

In order to obtain a constant mean terrain clearance, the aeromagnetic survey was flown by a "drape flying" technique 300 m above terrain. This procedure minimizes the loss of resolution and attenuation of anomalies due to variations in height over mountainous terrain when flying at a constant barometric altitude. Examination of altimetry data in a nearby quadrangle in the Brooks Range shows that survey aircraft commonly fall 75-150 m below the specified elevation over many ridges and fly 30-100 m above that elevation in valleys (Cady, 1978a) and thereby may distort some magnetic highs and lows. An amplification of magnetic highs has probably occurred where ridges are formed by magnetic rock, as in the belt of schists in the southern part of the quadrangle. Magnetic lows occur where valleys cut the schist belt. This distortion is mainly caused by deep erosion and subsequent sedimentary fill that has replaced magnetic bedrock in the valleys with nonmagnetic sediments.

METHOD OF INTERPRETATION

The aeromagnetic anomalies are caused mainly by variations in the percentage of magnetic minerals, primarily magnetite, in the underlying rock. Another factor, usually assumed to be of minor importance, is the intensity of natural remanent magnetization (NRM) in the magnetic minerals. Laboratory measurements made on samples from the schist belt in the Survey Pass quadrangle show average Konigsberger ratios (Q, the ratio of remanent to induced magnetization) between 5 and 26 (Table 1), indicating that NRM is an important factor there.

Previous aeromagnetic interpretations in the Brooks Range (Cady, 1978a,b; Hackett, 1980) were done without significant ground magnetic fieldwork. Prior to the 1978 field season of the Survey Pass AMRAP project, Hackett made a preliminary aeromagnetic-lineament map and Cady made a preliminary map showing inferred boundaries of magnetic rock units that might be inspected in the field.

During a three-week field season in 1978, Cady made 11 ground traverses (shown by dotted lines labeled 1a through 1k on Sheet 3; located in T. 20 N., R. 16, 17, and 23 E.; T. 21 N., R. 15, 18, and 25 E.; T. 23-24 N., R. 15 E.; and T. 26 N., R. 17 and 19 E. and plotted in fig. 1) aimed at locating magnetic rocks beneath interesting aeromagnetic anomalies. Total field magnetic measurements were made, generally at 30-m intervals, to locate the boundaries of magnetic rock units. High-amplitude, short-wavelength magnetic highs indicate the presence of magnetic rock at or near the surface. Identification of magnetic rocks was facilitated by a portable meter that could determine the magnetic susceptibility of rocks in place. The location of rocks with susceptibilities of at least 20×10^{-5} cgs is shown by station numbers on sheet 3.

At five of the sites with magnetic rocks, oriented cores were drilled for laboratory

Table 1.--Mineralogy and magnetic properties of selected rock samples

[All but the granite samples are from magnetic highs. Unit designation explained in table 2. Location of samples shown on sheet 3; for example, sample 01B comes from ST01 on sheet 3. Magnetic susceptibility is described as k(field), measured with a hand-held susceptibility meter, and k(lab), measured with a laboratory instrument. J_R is the remanent magnetization measured in the laboratory. Q is the mean Koenigsberger ratio; n.m., not measured.]

Rock type		Sample	Location		Mineralogy[1] of thin sections from magnetic sample site (in increasing order of abundance)	k(field) (10^{-5} cgs units)	No. of lab samples	k(lab) (10^{-5} cgs units)			J_R(lab) (10^{-5} cgs units)			
Unit	Description	No.	T. N.	R. E.				min	max	mean	min	max	mean	Q
Low- to intermediate-grade rocks of main schist belt														
Pz cs	Chloritoid-bearing schist.--Predominantly gray-weathering fine- to medium-grade chloritoid-bearing quartz muscovite schist. Chloritoid commonly occurs as stubby lath-shaped crystals as long as 1 mm. Contains glaucophane. Contains minor amounts of unit Pz qms.	01B	20	23	cld clt qtz mus schist	40-110	11	37	197	112	543	2445	1409	26
		03A	20	23	gnt clt mus alb qtz schist	~20	--	--	--	--	--	--	--	--
		04A	20	23	epi cld clt mus alb qtz schist	~20	--	--	--	--	--	--	--	--
Pz qms	Quartz muscovite schist.--Predominantly light-gray-weathering chlorite quartz muscovite schist, and porphyroblastic albite chlorite quartz muscovite schist. Locally differentiated into units Pz cs, Pz is, and Pz ca.	09A	19	17	gnt epi alb amp clt greenstone (within large area of Pz qms)	~20	--	--	--	--	--	--	--	--
		22A	20	16	epi gnt clt alb qtz mus schist	100-500	6	25	623	216	17	390	148	5.4
		38A	21	25	gnt clt qtz mus schist	n.m.	8	5	319	174	13	1741	411	4.9
		38B	21	25	gnt epi clt mus qzt schist	n.m.	--	--	--	--	--	--	--	--
		19A	19	16	gnt cal epi mus clt alb qtz schist (Pz ca calcareous subunit of Pz qms)	~20	--	--	--	--	--	--	--	--
Low- to intermediate-grade metamorphic rocks outside main schist belt.														
Pz clq	Chloritic quartzite and chloritic quartz schist.	28A	24	15	cal clt mus qtz quartzite		10	6	769	250	2	66	24	0.15
		28B	24	15	cal clt opq flu mus qtz schist	140-500	--	--	--	--	--	--	--	--
		28C	24	15	clt plg cal mus qtz quartzite		--	--	--	--	--	--	--	--
Low-grade metamorphosed sedimentary rocks														
Dc	Chlorite and chloritoid-bearing phyllite and semischist.--Light-green-weathering chloritic phyllite and chloritoid-bearing muscovite chlorite quartz semischist.	35	26	19	qtz bio cld schist (from X-ray spectrometer)	20-30	--	--	--	--	--	--	--	--
High-grade metamorphic rocks														
Pz sch	Schist.--Predominantly garnet biotite albite muscovite quartz schist. Includes minor muscovite quartzite, quartz muscovite schist, limestone, and greenstone.	36A-J	21	18	Most commonly ±gnt bio clt alb mus qtz schist	20-230	12	--	--	23	--	--	2	0.31
Granitic rocks														
Dgr	Arrigetch Peaks pluton.--Cataclastic granitic rocks.	44	23	21	Porphyroclastic bio mus granite	n.m.	8	2.2	3.1	2.6	0.03	0.37	0.15	0.11

[1]Petrography by S. W. Nelson. Mineral abbreviations:

alb	albite	cal	calcite	epi	epidote	mus	muscovite
amp	amphibole	cld	chloritoid	flu	fluorite	opq	opaque
bio	biotite	clt	chlorite	gnt	garnet	plg	plagioclase
						qtz	quartz

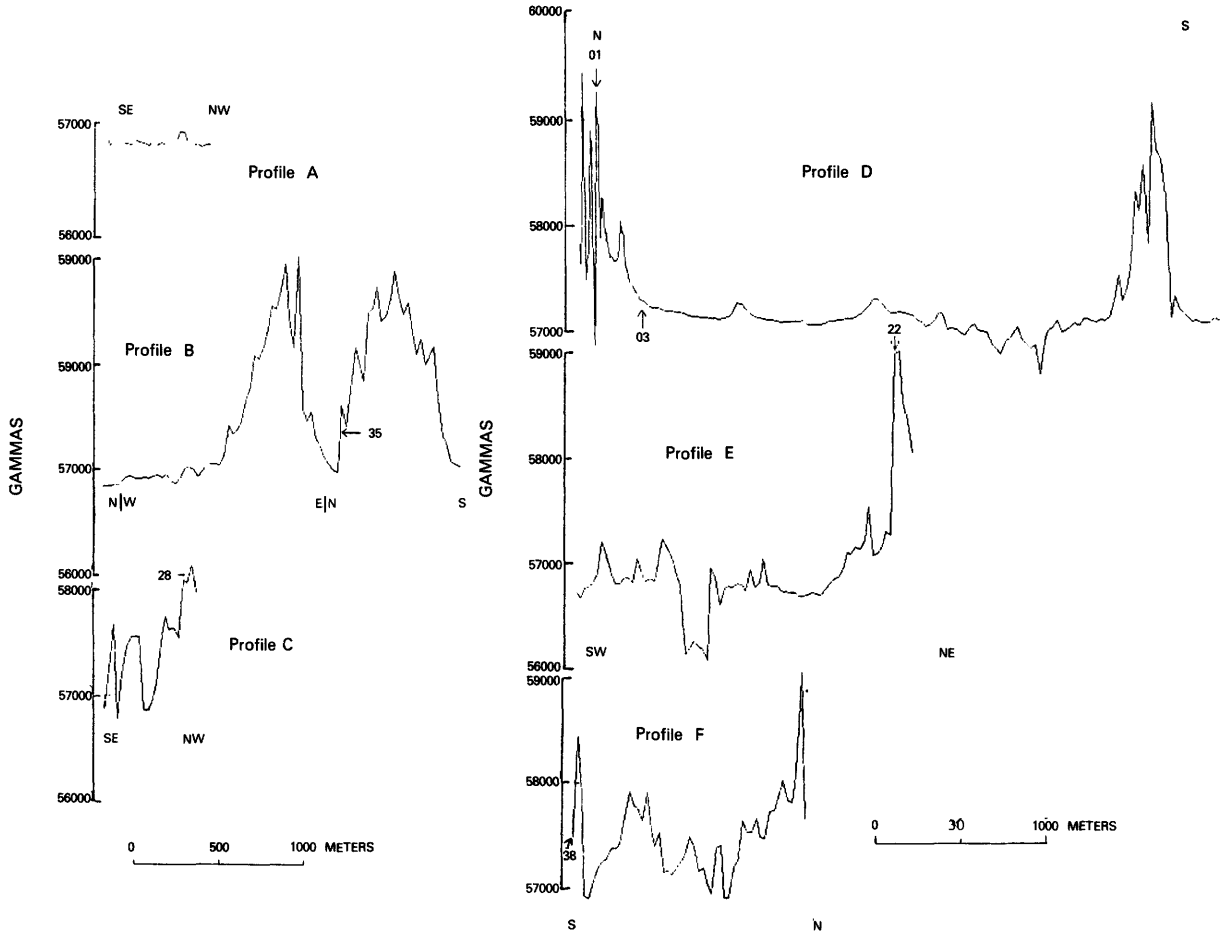

Figure 1.--Total field magnetometer profiles measured along tracks labeled 1a through 1k on sheet 3. Magnetometer sensor was approximately 3 m above the ground, and observations were made at intervals of 20 paces (approximately 30 m). High-amplitude, short-wavelength variations in the magnetic field indicate magnetic sources near the surface. Unlabeled numbers on the profiles are stations shown on sheet 3 and table 1. Changes in line direction shown by vertical bars.

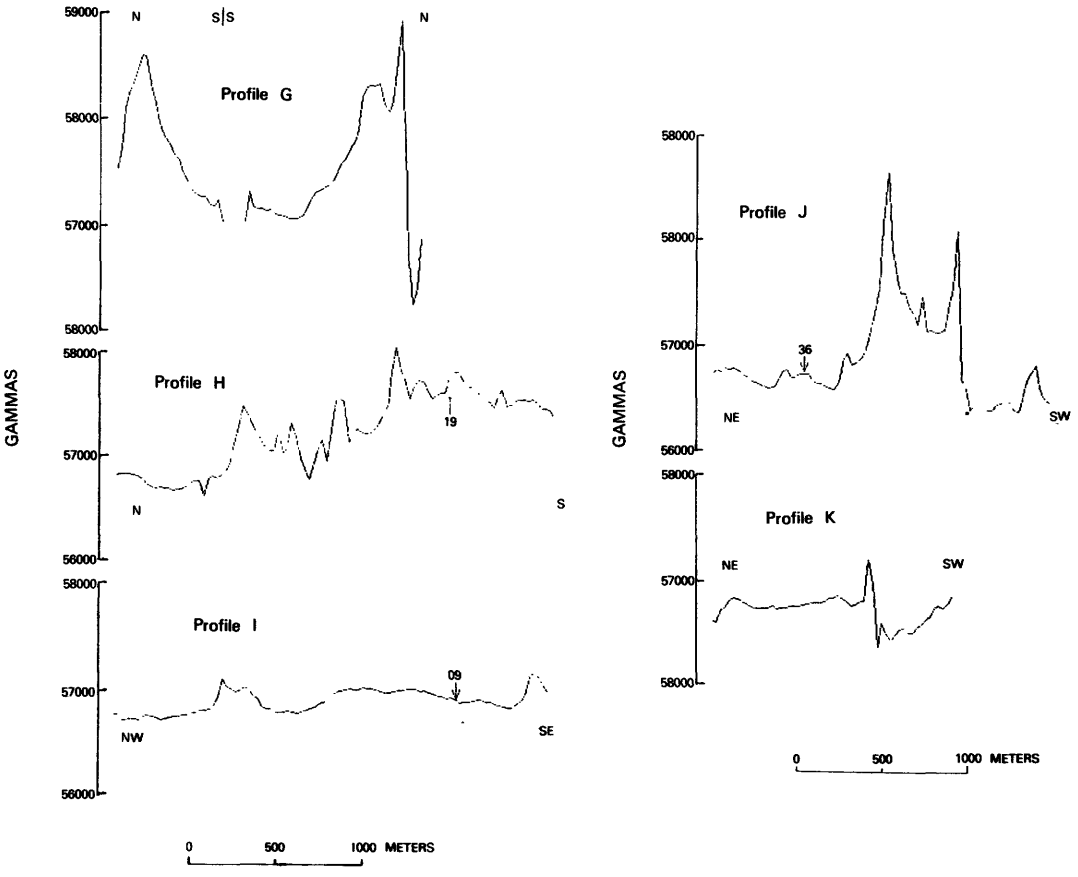

Figure 1.--(continued).

measurements of magnetic susceptibility and direction and intensity of natural remanent magnetization. Oriented cores were also drilled at a sixth site into a relatively nonmagnetic unit, the granite of the Arrigetch Peaks pluton. The magnetic-field directions obtained were scattered, even after cleaning by AC demagnetization, and deemed unreliable, but the susceptibility and remanent-magnetization-intensity measurements were consistent. They are given in table 1.

Axes of selected magnetic highs and lows were drawn on sheet 3 to show the linear continuity of certain anomalies. Local magnetic highs within each anomaly trend were labeled according to the rock type present at the site, which may cause the high.

Magnetic depth estimates made using the method of Vacquier and others (1951) showed that the maximum depth to most anomaly sources is 300 to 1200 m below the aircraft, so magnetic source rocks are either at the surface or less than 600 m deep.

Areas of inferred magnetic rock were outlined on sheet 3, following the zone of steep gradient surrounding magnetic highs. Contacts that may be exposed are shown by solid lines, and contacts that are probably deeply buried are shown by dashed lines. In some cases, a rock unit is outlined by two contacts that show its general three-dimensional configuration. A solid line shows its areal extent near the surface, whereas a dashed line shows its maximum lateral dimension at an approximate depth of several kilometers. For simplicity of presentation, solid inferred contacts are drawn across numerous valleys where steep magnetic gradients suggest that magnetic rock is continuous along strike beneath relatively thin sedimentary cover.

Magnetic anomalies are labeled with the symbol of the geologic unit used on the detailed geologic map of Nelson and Grybeck (1980). Table 2 is a correlation chart that shows the comparable units used on the generalized geologic base.

MAJOR MAGNETIC TERRANES, AND THE MAGNETIC ROCKS THEY CONTAIN

The aeromagnetic map has been divided into eight major terranes of differing magnetic character. The terrane boundaries generally do not coincide with surface contacts between magnetic and nonmagnetic rock. Magnetic boundaries may be faults, major unconformities, or intrusive contacts that separate, at depth, regions with different magnetic properties. The boundaries are indicated on sheet 3 by heavy, dashed lines.

Terrane I lies at the north border of the Survey Pass quadrangle in an area containing Devonian clastic sedimentary rocks, primarily the Kanayut Conglomerate, and abundant Quaternary alluvium. The terrane is defined by the south flanks of two broad magnetic highs having a maximum depth to source of about 10 km. The source rocks are part of a dense magnetic basement terrane, known only by its gravity and magnetic expression, that underlies much of the Arctic Slope of Alaska (Cady, 1978b, fig. 1).

Terrane II is defined by a broad (35 km) east-trending magnetic low that occurs over a large area containing primarily outcrops of the Devonian Hunt Fork Shale. The low is part of a magnetically quiet region that, from the available magnetic data (Decker and Karl, 1977), appears to run along the Brooks Range generally between the mountain crest and the magnetic basement terrane (I) from long 147° to long 156°. Published geologic sections (Mull and others, 1976; Nelson and Grybeck, 1980) show a thick sedimentary section in the vicinity of the magnetically quiet area, but they are ambiguous about the nature of the rocks occurring below the lower Paleozoic strata.

The noise of the available aeromagnetic data is too great to determine whether nonmagnetic basement or very deep magnetic basement is the cause of the magnetic quiet region. The thickness of the sedimentary section cannot easily be determined from available gravity data, because the gravity low caused by the sedimentary rocks is inseparable from the gravity low caused by the inferred isostatic root of the Brooks Range.

Within terrane II occur a series of 10- to 20-km-wide north-trending magnetic highs and lows with peak to trough amplitudes between 5 and 20 gammas. The origin of these anomalies is unknown. They may be spurious artifacts of the data collection and reduction process, or, if they are real, they could result from suprabasement relief in a weakly magnetic basement 5-10 km deep.

LeCompte (1981) has inferred, from circular features observed on Landsat images, that two large buried plutons may be present in terrane II. The aeromagnetic data neither disprove nor support this hypothesis; felsic plutons commonly are magnetically featureless (for example, Paleozoic granite in T. 24 N., R. 26 E., just within terrane II), but the magnetic map shows no circular or arcuate features in terrane II which might represent contact aureoles or any other magnetic effect around the inferred plutons.

Terrane III occurs as a 4-km-wide linear band of magnetic highs (Hl) with amplitudes of as much as 150 gammas. The terrane coincides with an east-trending region of calcareous phyllite bounded by north-dipping thrust faults. The band of anomalies is best defined in the center of the quadrangle, where it is apparently caused by a magnetic part of the chlorite- and chloritoid-bearing phyllite and semischist unit. It is uncertain whether the band of anomalies could be extended to the east (Hl??), where the surface rocks are primarily mapped as orange dolomitic marble (including the Skajit Limestone) or to the west (Hl?), where

Table 2.--Correlation of geologic map units used to label magnetic highs and lows. Interpreted magnetic intensities decrease downward within each group listed below

Detailed geology, (Nelson and Grybeck, 1980)		Generalized geology, (Nelson and Grybeck 1981)	
Mostly in magnetic terrane VI			
Quartz muscovite schist	Pz qms	Low-grade schist	Pz s
Chloritoid-bearing schist	Pz cs		
Iron-stained schist (probably equivalent to Pz qms and Pz cs)	Pz is		
Undifferentiated schist (mostly Pz qms)	Pz us		
Calcareous schist (equivalent to Pz qms)	Pz ca		
Mostly in magnetic terrane IV			
Undifferentiated schist and paragneiss	Pz sgn	Low- to medium-grade schist and gneiss	Pz sgn
Mixed schist and marble with skarns near Arrigetch Peaks pluton	Pz msm		
Schist (higher grade equivalent to Pz qms to south)	Pz sch		
Chlorite quartzite and chloritic quartz schist	Pz clq	Chlorite quartzite and chloritic-quartz schist.	Pz clq
Skajit Limestone with skarns near Arrigetch Peaks pluton	DSsk	Skajit Limestone and orange marble	DSs
Orange dolomitic marble	DSso		
Greenstone and greenschist	Pz gg	Mafic volcanic and intrusive rocks	Pz m
Mostly in magnetic terrane III			
Chlorite-and chloritoid-bearing phyllite and semischist	Dc	Calcareous phyllite	Dp
Ferruginous calcareous metasedimentary rocks	Dfc		

the ferruginous, calcareous metasedimentary rock unit has been mapped.

Surface magnetometer profiles across anomaly H1 (in T. 26 N., R. 17 E. and R. 19 E.) are shown in fig. 1, profiles a and b. They show that the source has an outcrop width of only 300 to 400 m, coincident with the line showing the anomaly crest on sheet 3. In contrast, the probable surface contacts of the magnetic source, inferred from steep magnetic gradients on the aeromagnetic map, outline a unit 2 to 2.5 km wide. Apparently, the resolution of the aeromagnetic data is inadequate precisely to define the surface configuration of magnetic rocks. Hence, everywhere on the aeromagnetic interpretation map, the boundaries of areas inferred to include exposures of magnetic rock are only approximate.

High H1 is symmetrical, especially if adjustments are made to allow for the interfering effect of high H2f, to the south. A symmetrical high trending at right angles to magnetic north might be caused by a slab dipping north, parallel to the Earth's magnetic field. In fact, the geologic map of the area shows a number of north-dipping thrust sheets.

This tentative interpretation was tested by two-dimensional magnetic modeling along line A-A', shown on figure 2. A linear regional trend, interpolated between a value of -110 gammas assumed south of H1 in the absence of H2f and a value of -120 gammas observed in the low north of high H1, was added to the calculated values. The source body was assumed to crop out only in the 380-m-wide band identified in the ground magnetometer profile (fig. 1b). About 50 models were tested, using an interactive graphical magnetic modeling program (Cady, 1980; Shuey and Pasquale, 1973). The range of acceptable models is shown in the bottom part of figure 2. There is little control on the depth extent of the source, although the lowest root-mean-square error between observed and calculated magnetic field was obtained by assuming a bottom depth of 2 km. Acceptable models had steep (80^{o}-90^{o}N.) south boundaries and north boundaries that dip between 30^{o} and 55^{o} N. The model is consistent with the moderately dipping thrust fault mapped at the boundary the magnetic source to the north. The steeper boundary on the south differs from the measured dips of 45^{o}-50^{o} N. The discrepancy may be caused by interference from H2f, which made the south flank of H1 difficult to model.

The zone of high magnetic relief determined by ground profiles in terrane III contained nonmagnetic ($k<10x10^{-5}$ cgs) chloritic phyllite at the surface. One magnetic sample (at station 35, T. 26 N., R. 19 E.), a very friable sheared green quartz-biotite-chlorite schist, has a susceptibility of $20\text{-}30x10^{-5}$ cgs--about half that required to cause the observed magnetic high. Magnetiferous chlorite schist at depth is inferred to be the source of H1.

Terranes IV and V contain metamorphic and plutonic rocks in the core of the Brooks Range. The exposed plutons are marked by magnetic lows, and other magnetic lows are used to infer buried plutons. The continuity of the magnetic lows between the Mount Igikpak and Arrigetch Peaks plutons suggest that the plutons are continuous at depth. The pattern of subdued magnetic highs over the metamorphic rocks is irregular. Some anomaly trends are subparallel to the pluton boundaries, a correlation that suggests either contact metamorphic aureoles or magnetic units deformed by the tectonic emplacement of the plutons. The boundaries between terranes IV and V are uncertain, because they separate subtle highs from lows.

Terrane V is the magnetically low-intensity and quiet terrane associated with the nonmagnetic Mount Igikpak and Arrigetch Peaks plutons. A similar terrane is suspected southeast of the Arrigetch Peaks (terrane V?) where an equally low-intensity and quiet magnetic field suggests the presence of plutonic rocks at depth. The boundary between terranes IV and V? correlates well with the outer boundary of the zone of amphibole-bearing schists on the metamorphic map (Nelson and Grybeck, 1981), between R. 17 E. and the east edge of the quadrangle. Terrane V??, northwest of Mount Igikpak, is also magnetically low and quiet, but it lies in a different structural domain (Grybeck and Nelson, 1981a) and in a zone of lower metamorphic grade (Nelson and Grybeck, 1981) than either the known plutons or the metamorphic rocks that surround them. Other evidence that terrane V?? is anomalous, perhaps that it contains a buried pluton, is the presence of a circular feature visible on Landsat images (LeCompte, 1981). Alternatively, the magnetic low of terrane V?? and possibly that of terrane V? may be caused by a very thick section of Skajit Limestone.

Terrane IV is characterized by irregularly shaped highs (labeled H2a through H2t) with typical amplitudes of 50 to 130 gammas, although H2d has a peak to trough amplitude of 274 gammas. The anomalies of terrane IV do not exhibit the linearity and continuity of anomalies in terranes III and VI, and they cannot be explained by a single rock type or geophysical cause. The authors are not satisfied with their explanations for the anomalies in terrane IV, and the reader should regard the explanations that follow as untested hypotheses.

Magnetic highs and lows that wrap around plutons are commonly explained by the formation or destruction of magnetite in country rock by contact metamorphism. Comparison of the geologic and aeromagnetic maps shows that metamorphic rock units associated with magnetic highs (especially highs H2j, H2g, H2r, H2o, H2p, H2t, and H2s) adjacent to the Arrigetch Peaks and Mount Igikpak plutons are "mixed schist and marble", "schist and paragneiss", "schist", "chloritic quartzite and chloritic quartz schist", and a single occurrence of "quartz muscovite schist". Many of the rocks in the vicinity of the plutons are higher grade equivalents of rocks found elsewhere in the quad-

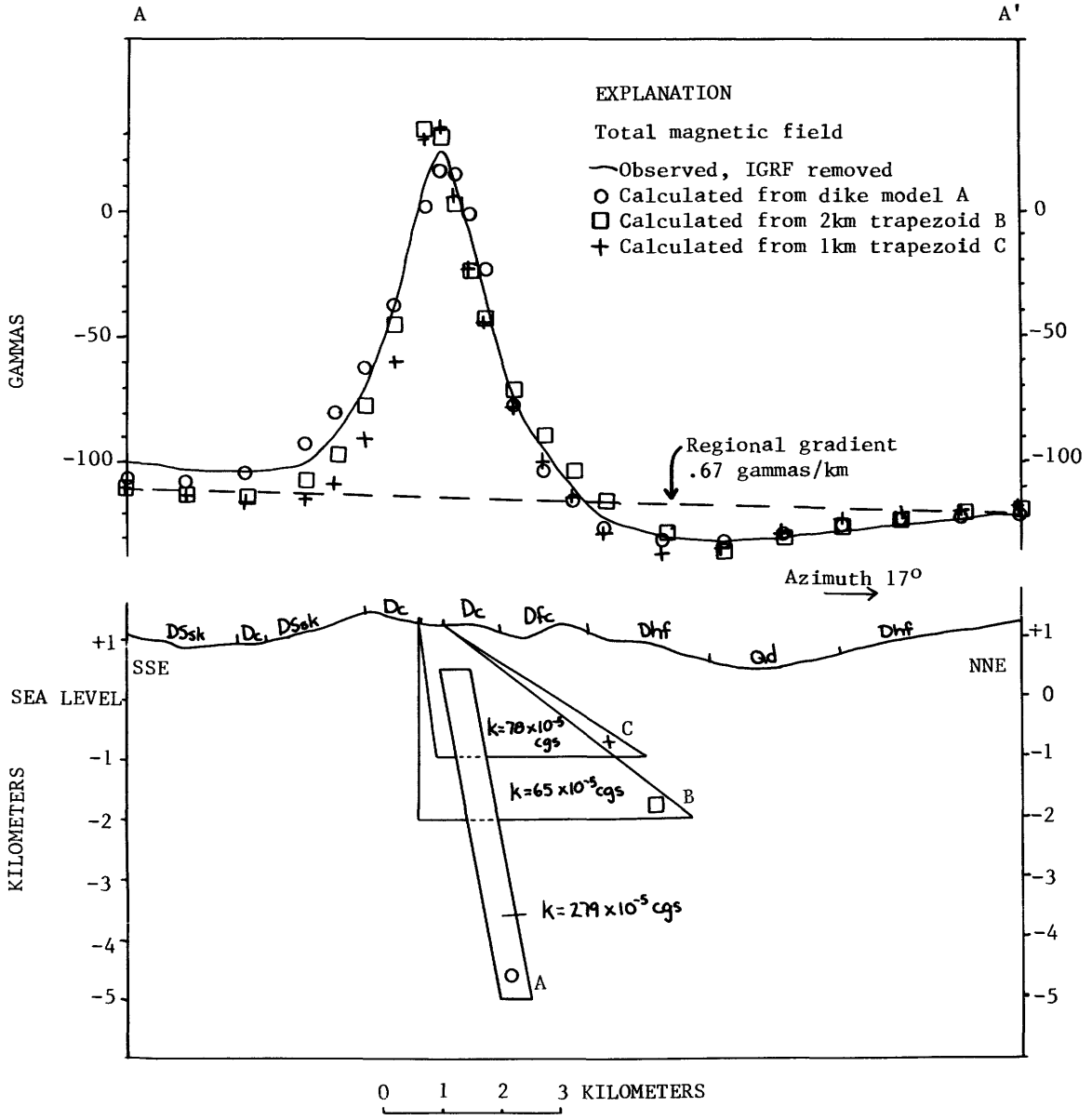

Figure 2.--Two-dimensional model along profile A-A' that explains the linear magnetic high in the thrust belt (terrane III) north of the Brooks Range. Symbols are superimposed on the line that shows the observed total magnetic field to show the field calculated from each of three hypothetical source bodies. Magnetic susceptibility (k) measured in cgs. Inclination and declination of the Earth's magnetic field are 77° and 25°, respectively. Flight-line elevation assumed to be 305 m (1000 ft) above terrain. Geology generalized from Nelson and Grybeck (1980). Rock-type symbols are explained in table 2, except Dhf (Hunt Fork Shale) and Qd (Quaternary deposits).

rangle, but as the plutons are interpreted to be tectonically emplaced (Nelson and Grybeck, 1981), contact metamorphism is not expected to be a cause for the magnetic highs. One exception to this generalization is a magnetite-bearing skarn that occurs near H2j, southeast of the Arrigetch Peaks pluton (Nelson and Grybeck, 1980). The most likely explanation for magnetic highs near the plutons is that they result from variations in original magnetic composition whose shapes have been altered by deformation and possible metamorphism caused by the emplacement of the plutons.

Other highs, such as H2i, H2l?, and H2m?, occur in areas where the orange dolomitic marble unit and Skajit Limestone crop out east of the plutons. It is not known whether the highs are caused by magnetic zones of greenstone and greenschist within these carbonate units or by magnetic lithologies that underlie the carbonate rocks. Either could result from contact metamorphism near the perimeter of the plutons. Highs H2i and H2h? are particularly puzzling, because they constitute a 15-km-wide zone of magnetic highs situated entirely within carbonate rocks. The zone is contiguous with mapped and inferred plutons only along its southwest margin. The parallel arrangement of anomaly trends H2i and H2h? suggests that the magnetic source rock may be a stratabound unit contained in folds with axes parallel to the anomaly trends.

The geologic significance of other anomalies in terrane IV is generally unknown. High H2k? (T. 23 N., R. 26 E.) is caused by rock buried as much as 3 km or more. High H2d (T. 23 N., R. 15 E.) has an amplitude of more than 200 gammas and is surrounded by a well-developed string of lows (L1) that suggests that the source has shallow roots. Field observation at station 28 (T. 24 N., R. 15 E.) showed that H2d is caused by chloritic quartzite and chloritic quartz schist. Possibly one or more of highs H2b, H2c, H2e, and H2f (all in the west-central part of the quadrangle), irregular in shape like H2d but with amplitudes of only 30 to 100 gammas and gentler gradients, are caused by buried bodies of chloritic quartzite or chloritic quartz schist. Steep gradients on the north side of H2c suggest that the source rocks dip south, whereas steep gradients on the south side of H2b suggest that the source rocks dip north. Perhaps the magnetic source rocks occur in a syncline with its axis between the highs and the limbs under the highs. Outcrops of the greenstone and greenschist unit at H2b may be part of the source body.

Lows R1 (T. 24 N., R. 16 E.) and R2 (T. 24 N., R. 18 E.), with depths of 80 and 50 gammas, respectively, are somewhat isolated from neighboring magnetic highs. They may be caused by reversely magnetized rock of unknown type.

Terrane VI traverses the southern part of the quadrangle and coincides with the low- to intermediate-grade belt of schists and associated metamorphic rocks of the southern Brooks Range. This so-called "schist belt" produces a regional magnetic high 5-15 km wide with a typical amplitude of 300 gammas above the low to the south and 250 gammas above lows to the north. Local highs with amplitudes of as much as to 500 gammas occur where magnetic quartzite forms resistant ridges.

Magnetic highs in the schist belt are associated with mapped occurrences of the quartz-muscovite schist unit (locally divided into the calcareous schist, iron-stained schist, and undifferentiated schist subunits, and the chloritoid-bearing schist unit. Six ground magnetometer traverses were made in the schist belt. Rock samples magnetic enough to cause the observed highs were obtained at station 01 (T. 20 N., R. 23 E., fig. 1, profile d), in a resistant peak of chloritoid-bearing chlorite-quartz-muscovite schist and at station 22 (T. 20 N., R. 16 E., fig. 1, profile e) and station 38 (T. 21 N., R. 25 E., fig. 1, profile f) in peaks along resistant ridges of chlorite-quartz-muscovite schist. Elsewhere, although ground magnetometer profiles indicated that highly magnetic rocks were present within 30 to 50 m of the surface, the outcropping rocks were friable and eroded, and rocks with magnetic susceptibility greater than 20×10^{-3} cgs could not be found.

Although the regional high associated with the schist belt is continuous across the width of the quadrangle, the high crest of the anomalies is subdued over the valleys of Mauneluk River, Beaver Creek, Reed River, Walker Lake, Alatna River, Tobuk Creek-Iniakuk Lake, and Iniakuk River. Massive erosion in these glaciated valleys has apparently removed a significant quantity of magnetic rock that, in the ridges to either side, causes the high-amplitude, shorter wavelength components of the anomaly trend.

Magnetic highs in terrane VI commonly have steep gradients in the north and more gentle gradients in the south. Although the source bodies are obviously very complex, the gradients suggest the magnetic rocks are bounded by steep (north-dipping?) contacts to the north and irregular, generally south-dipping contacts to the south.

In the western part of the schist belt, the magnetic highs caused by quartz-muscovite schist (H3a-H3f) occur in paired, east-trending arcuate belts surrounding a low labeled L2. In T. 20 N., R. 13 and 14 E., L2 lies close to the axis of the Kalurivik arch (Grybeck and Nelson, 1981a). Farther east, in T. 20 N., R. 16 E., L2 coincides with narrow exposures of granite elongate parallel to the low. We conclude, therefore, that the granite occurs in the core of the Kalurivik arch and that the axis of the arch extends east along L2 at least to T. 20 N., R. 16 E., and possibly into T. 20 N., R. 17 E.

The high-amplitude elongate magnetic highs of the schist belt are markedly different from the broad magnetic lows over the Mount Igikpak and Arrigetch Peak plutons. There is no magnetic evidence that the small granite exposures

in L2 are connected at depth with the larger plutonic complexes to the north.

Most of the rocks mapped within L2 are quartz-muscovite schists similar to those occurring in the adjacent highs, although the metamorphic map (Nelson and Grybeck, 1981) shows a zone of higher grade around the granitic rocks in T. 20 N., R. 16 E. Two explanations are possible. One is that the magnetic quartz-muscovite schist occurs in a contact aureole surrounding a buried pluton. The other is that metamorphism around the pluton has destroyed magnetite in previously magnetic quartz-muscovite schist. In either case, the aeromagnetic map suggests that a buried pluton forms the core of the Kalurivik arch all along L2.

High H3b has a steeper magnetic gradient on its north flank than on its south flank. This could indicate that the quartz-muscovite schist that causes the high dips to the south, and that the Kalurivik arch is overturned to the north. This interpretation is speculative on the basis of the magnetic anomaly alone, because the shape of H3b is strongly dependent upon the configuration of the inferred pluton under L2. It is confirmed, however, by the geologic map of Nelson and Grybeck (1980).

The north flank of highs H3a, H3b, and H3c coincides with the so-called Walker Lake lineament (see Grybeck and Nelson, 1981a). The arcuate shape of the magnetic gradient bounding the highs suggests that the north contact of the magnetic schist has been folded. A discontinuity labeled F1 between H3a and H3b may result from faulting of the folded contact.

Between the Kalurivik arch and Walker Lake, a single line of subdued highs (H3g) is probably caused by a south-dipping unit of magnetic schist.

East of Walker Lake the anomaly pattern again doubles, but this time in an erratic way suggestive of faulting. A steep gradient zone labeled F2 forms the north flank of H3h. Low L3 occurs over the Skajit Limestone to the north of the gradient zone. Because it is so straight in an otherwise arcuate terrane, and because it separates two different rock types, gradient zone F2 probably marks a high-angle fault. It coincides with a mapped thrust fault in T. 20 N., R. 22-23 E. and provides strong evidence that the fault, which is also part of the so-called Walker Lake lineament, continues east-northeast to T. 21 N., R. 24 E.

The string of subdued highs labeled H3i, north of L3, appears to be caused by quartz-muscovite schist, but it is in an area of abundant limestone. It coincides with a tongue of low-grade metamorphic rocks (T. 21 N., R. 22-24 E.) within higher grade rocks on the metamorphic map (Nelson and Grybeck, 1981). Magnetic modeling, discussed below, shows that the source of the southern high (H3h) dips south. It is possible that the sources of H3h and H3i are the limbs of an anticlinorium that has been disrupted by faulting along line F2. In any case, line F2 marks an important lithologic break between schists to the south and abundant carbonate bodies to the north.

Figure 3 shows a magnetic model along profile B-B' for H3h in the schist belt. The shorter wavelength details of the high (the peak and a bump on the north flank) were ignored, and the top of the source body was held about 1 km below the surface in order to model the deeper configuration of the source body, which is assumed to be the chloritoid-bearing schist unit. The south contact of the source dips about 55^{o} south. Remanent magnetization directions at the site (station 01) were very scattered, so we assumed randomization of remanent magnetization, with direction determined by induction parallel to the Earth's magnetic field. The magnetization required in this direction to match the observed anomaly, using the best-fit geometry shown in figure 3, was 208×10^{-5} cgs. This value is much less than the mean remanent magnetization of 1409×10^{-5} cgs measured at site 01. Hence, the magnetic source body may be smaller than that shown in figure 3, have non-uniform magnetization intensity, or have a variable remanent magnetization direction that yields a net vector intensity less than the mean scalar intensity.

North of the main high (H3h), profile B-B' crosses a subdued magnetic high (H3i) in T. 21 N., R. 22 E. No attempt was made to model the subdued high because its form is poorly defined, and it is inseparable from the polarization low, caused by the dipole nature of magnetic sources, that occurs north of the main high. In figure 3, the calculated field north of the magnetic source body is lower by nearly 100 gammas than the observed field, which includes the subdued high. Because of interference from the adjacent subdued high, the north boundary of the source body is poorly defined.

The magnetic highs in the schist belt do not correlate with details of the mapped geology. Although there are strong correlations between magnetic highs and the quartz-muscovite schist unit and the chloritoid-bearing schist unit, many mapped exposures of both of the units occur far from magnetic highs. It would be very interesting to do detailed geologic mapping of a part of the schist belt, concurrently measuring magnetic susceptibility of the rocks to define magnetic units and using the aeromagnetic map as a guide to extrapolating unit boundaries between traverses.

Terrane VII is a broad magnetic low of about 50 gammas that coincides with a topographic low (the Kobuk trench) that contains the Kobuk fault system of Grantz (1966) and Patton (1973). We interpret the low as a normal polarization low caused by the contrast between nonmagnetic Paleozoic phyllite and Quaternary sediments in the Kobuk trench and magnetic rocks to the north and south.

Terrane VIII occurs only in the southeast corner of the quadrangle. It is part of a major aeromagnetic high associated with mafic and ultramafic rocks of the Angayucham Mountains in

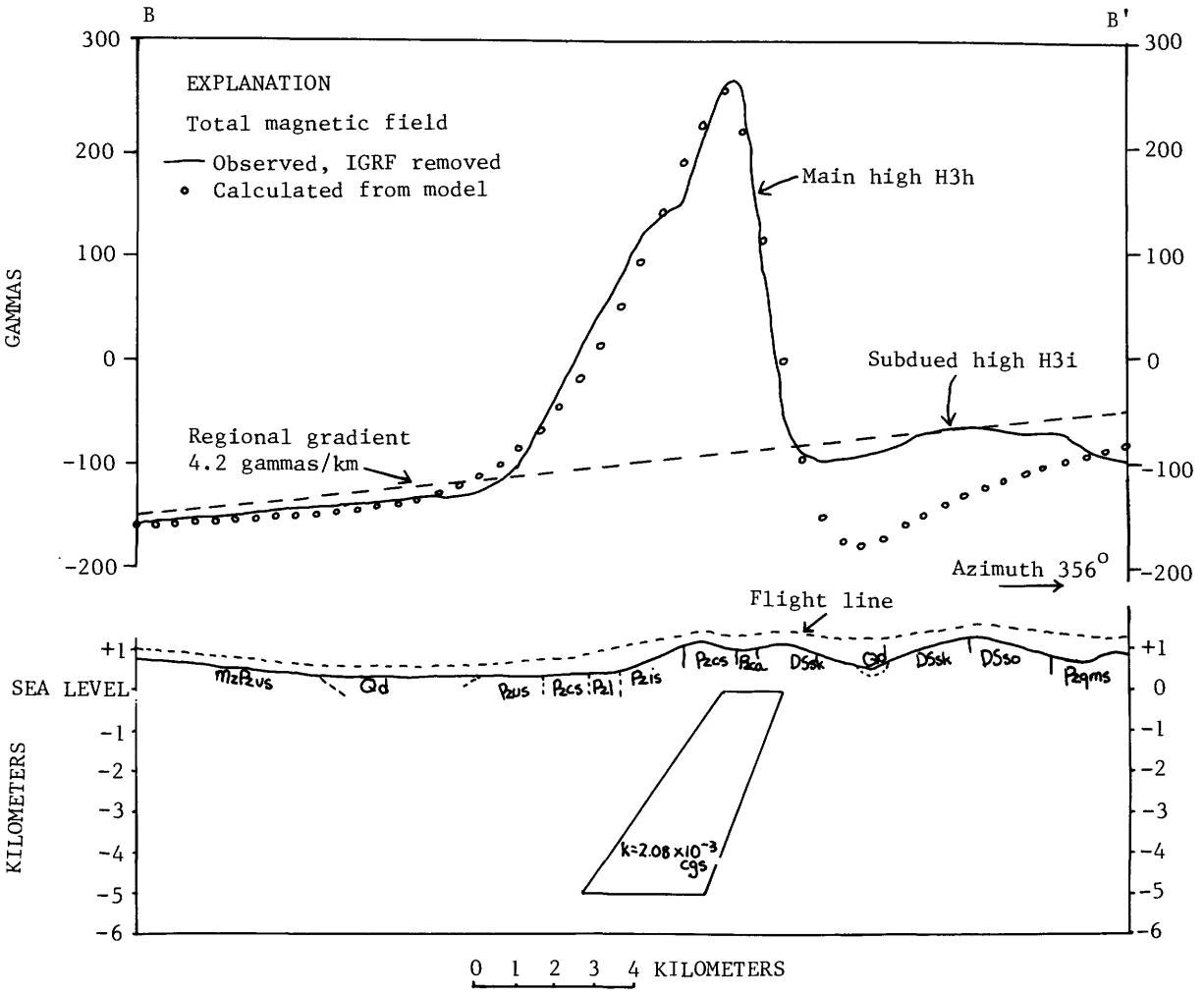

Figure 3.--Two dimensional model along profile B-B' that explains the magnetic high over the southern Brooks Range schist belt. The regional gradient, chosen by inspection of the aeromagnetic map past the ends of the profile, was added to the calculated values. Magnetic susceptibility (k) measured in cgs. Inclination and declination of the Earth's magnetic field are 77° and 25°, respectively. Flight-line elevations were estimated from radar altimetry and varied from less than 150 m to more than 400 m above terrain. Geology generalized from Nelson and Grybeck (1980). Rock-type symbols are explained in table 2, except MzPz vs (mafic volcanic rocks, phyllite, sandstone, and chert), and Qd (Quaternary deposits).

the Hughes and Shugnak quadrangles to the south.

IMPLICATIONS FOR MINERAL RESOURCE ASSESSMENT

In terranes I and II, magnetic basement is at least 5 km deep, and the magnetic contours show no evidence of metamorphic aureoles, so mineral deposits associated with crystalline rocks are not expected.

Terrane III contains only one known mineral deposit; placer gold found in T. 27 N., R. 13 E. at the west end. According to Grybeck and Nelson (1981b), the source may be pyrite-quartz veins cutting phyllite. In the Chandalar district, there is a regional association of gold with magnetic highs, probably caused by greenstone (Cady, 1978a). If the mineralization is associated with the magnetic rock of terrane III, there could be gold prospects elsewhere in the terrane.

In terranes IV and V, very few mineral prospects in the map of Grybeck and Nelson (1981b) are close to magnetic highs. The exceptions are mineralized skarns (prospects 50-54) near H2j, a mineralized granite contact (30) near H2g, mineralized calc-silicate rock (49) at H2o, and anomalous beryllium (45) at H2p. These examples suggest that the magnetic highs peripheral to terrane V might be associated with contact-metamorphic skarns, some of which may be mineralized. It must be noted, however, that mineralized skarns found to date are too small to cause anomalies visible on the aeromagnetic map (sheet 1). Most of the magnetic highs in terranes IV and V remain unexplained.

Within terrane IV, sulfide mineralization of the Ambler district is found as far east as Walker Lake. The mineralization occurs in a belt of felsic metavolcanic schists (Sicherman and others, 1976) that are generally accompanied by magnetic lows (Gilbert and others, 1977). The Picnic Creek deposit (no. 68 in the mineral deposits map, Grybeck and Nelson, 1981b) is a good example of such a deposit in the Survey Pass quadrangle. It occurs in felsic volcanic rocks that are delineated by L3, a linear saddle between magnetic highs. Elsewhere in the schist belt, saddles between magnetic highs are worth investigating for the presence of felsic volcanic rocks and potentially associated mineralization.

REFERENCES

Alaska Division of Geological and Geophysical Surveys, 1976, revised 1979, Aeromagnetic survey of Survey Pass quadrangle, Alaska: Scale 1:63,360.

Cady, J. W., 1978a, Aeromagnetic map and interpretation, Chandalar quadrangle, Alaska: U.S. Geological Survey Miscellaneous Field Investigations Map MF-878-C, scale 1:250,000.

_____1978b, Aeromagnetic map and interpretation of the Philip Smith Mountains quadrangle, Alaska: U.S. Geological Survey Miscellaneous Field Investigations Map MF-879-E, scale 1:250,000.

_____1980, Calculation of gravity and magnetic anomalies of finite-length right polygonal prisms: Geophysics, v. 45, p. 1507-1512.

Decker, John, and Karl, Susan, 1977, Preliminary aeromagnetic map of the Brooks Range and Arctic Slope, Alaska: U.S. Geological Survey Open-File Report 77-166-E, scale 1:1,000,000.

Gilbert, W. G., Wiltse, M. A., Carden, J. R., Forbes, R. B., and Hackett, S. W., 1977, Geology of Ruby Ridge, southwestern Brooks Range, Alaska: Alaska Division of Geological and Geophysical Surveys, Geologic Report 58.

Grantz, Arthur, 1966, Strike slip faults in Alaska: U.S. Geological Survey Open-File Report 66-53, 82 p.

Grybeck, D., and Nelson, S. W., 1981a, Map and interpretation of the structural geology of the Survey Pass quadrangle, Brooks Range, Alaska: U.S. Geological Survey Miscellaneous Field Investigations Map MF-1176-B, scale 1:250,000.

_____1981b, Mineral deposits map of the Survey Pass quadrangle, Brooks Range, Alaska: U.S. Geological Survey Miscellaenous Geologic Investigations Map MF-1176-F, scale 1:250,000.

Hackett, S. W., 1977, revised 1980, Aeromagnetic map of southwestern Brooks Range, Alaska: Alaska Division of Geological and Geophysical Surveys, Geologic Report 56, scale 1:250,000.

_____1980, Aeromagnetic interpretation maps of the Ambler River quadrangle, Alaska: U.S. Geological Survey Open-File Report 78-120K, scale 1:250,000.

LeCompte, J. R., 1981, Maps showing interpretation of Landsat imagery of the Survey Pass quadrangle, Brooks Range, Alaska: U.S. Geological Survey Miscellaneous Field Investigations Map MF-1176-H, 2 sheets, scale 1:250,000.

Mull, C. G., Tailleur, I. L., Mayfield, C. F., and Pessel, G. H., 1976, New structural and stratigraphic interpretations, central and western Brooks Range and Arctic Slope: U.S. Geological Survey Circular 733, p. 24-26.

Nelson, S. W., and Grybeck, D., 1980, Geologic map of the Survey Pass quadrangle, Brooks Range, Alaska: U.S. Geological Survey Miscellaneous Field Investigations Map MF-1176-A, 2 sheets, scale 1:250,000.

_____1981, Map showing distribution of metamorphic rocks in the Survey Pass quadrangle, Brooks Range, Alaska: U.S. Geological Survey Miscellaneous Field Investigations Map MF-1176-C, scale 1:250,000.

Patton, W. W., 1973, Reconnaissance geology of the northern Yukon-Koyukuk province,

Alaska: U.S. Geological Survey Professional Paper 774-A, 17 p.

Shuey, R. T., and Pasquale, A. S., 1973, End corrections in magnetic profile interpretation: Geophysics, v. 38, p. 507-512.

Sichermann, H. A., Russell, R. H., and Fikkan, P. R., 1976, The geology and mineralization of the Ambler District, Alaska: Pacific Northwest Metals and Minerals Conference (AIME), Coeur d'Alene Idaho.

Vacquier, V., Steenland, N. C., Henderson, R. G., and Zietz, Isidore, 1951, Interpretation of aeromagnetic maps. Geological Society of America Memoir 47, 151 p.